RC2, Anonymous (main comments)

The submitted manuscript provides rigorous analysis on wave-current driven ripple development in cohesive clay bed. The analysis is based on a series of laboratory experiments. The discussed topic is interesting and important to advance our understanding of coastal morphodynamics.

We are grateful for the Reviewer's positive feedback regarding our contributions to the field of coastal morphodynamics. Please note that we have incorporated revisions into the manuscript in response to your feedback. The modified sections are now highlighted in red for your convenience.

(1) However, I find it difficult to read this paper. The main reasons of the difficulties in reading this paper are mainly associated with too many presented numeric and abbreviation when things are explained in the result section.

We will add a nomenclature list for readers to more easily understand the symbols. In addition, since equilibrium time, T_η and T_λ, are not really relevant to the discussion section, we have streamlined their mention in section 3.1 and instead stated that they show similar trends to the Wu et al. (2022) results.

[L208-220: '…, small ripples appeared at t = 10 min. Thereafter, ripple dimensions developed gradually over a period of around seven hours, stabilising to an equilibrium height and wavelength of 13.9 and 137 mm (Figure 3e and f). The equilibrium ripples retained … At C_0 = 10.8% (WC2), small ripples again appeared at t = 10 min and grew to equilibrium dimensions of η_e = 5.6 mm and λ_e = 125 mm. The small ripples formed at C_0 = 10.8% (WC2) were three-dimensional with discontinuous, sinuous crestlines in plan view. In cross-section, these ripples were asymmetric and flatter, with RSI = 1.6 and RS = 0.04 (Figure 4e, Table 2). The general trends in T_η and T_λ with C_0 were similar to those found by Wu et al. (2022). For the C_0 = 16.3% (WC2) case, the bed …']

(2) In addition, the authors refer earlier studies regarding experiment set-up and results from Wu et al. (2022). I often get lost what the main messages are in the texts or figures. Thus, some clarifications and rework in writing are needed before publication. I suggest the author focus on telling the main messages from their experiments and each figure in the revised manuscript. I also have some concerns about configurations of their experiment.

In order to improve readability, we have revised section of results to reduce numbers and symbols as mentioned above to address the reviewer's concern in RC2.1. Additionally, we have restructured both introduction and conclusion for clarity (see the end of this document). Furthermore, we will move the 3D phase diagram and text to a new section (4.4 Bedform phase diagrams) at the end of the discussion section based on L456-478. This will leave two paragraphs: L450-455 and L479-488 in a shortened implications section with the same title. We also will swap sections 4.3 and 4.2, so that the threshold of motion leads on to the phase diagram, and we finish on the most important point according to both the Reviewers and the order is consistent with the abstract and conclusions. Also, that way our reduction in hydraulic conductivity argument then relates back more immediately to the sudden drop in steepness discussed in section 4.1.

We have updated figures for clarification. We have changed 'initial' to (pre-) in Figures 5a-d and added (post-) to Figures 5e-k, so that the terminology is consistent with the caption. However, it is important to stress that Figures 5f-h are the pre-experiment cores for WC2 (L252). To emphasise this point, we have added the depth-mean post-experiment value in blue for Figures 5f-g, as this represents C_0 values for Figure 5i-k.

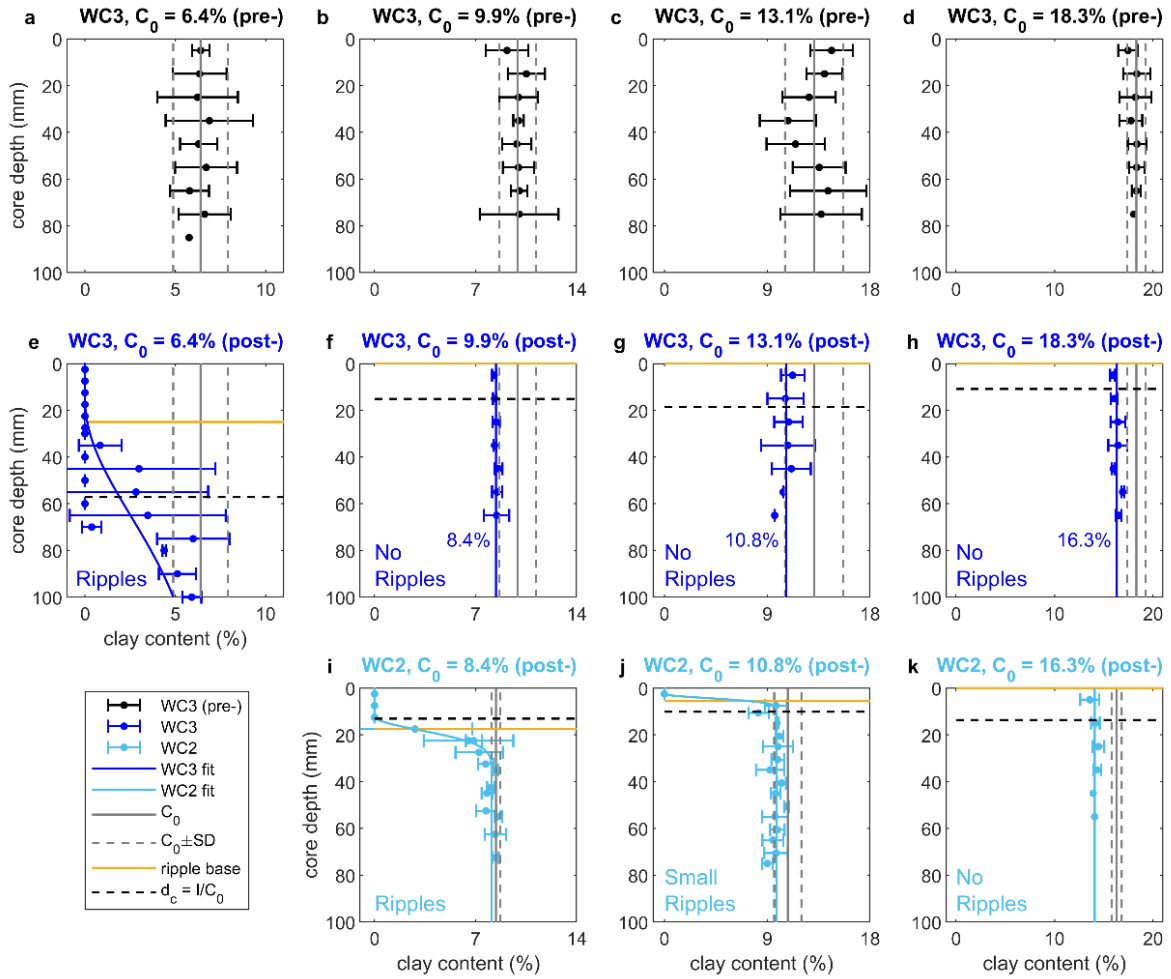

We also have reduced the legend to the three colours representing WC1–WC3 in Figure 8, explained the different symbols without abbreviations in the figure caption instead and labelled the two main groupings: ripples and no ripples. In addition, for clarity the caption no longer lists the values of C_0 for WC1.

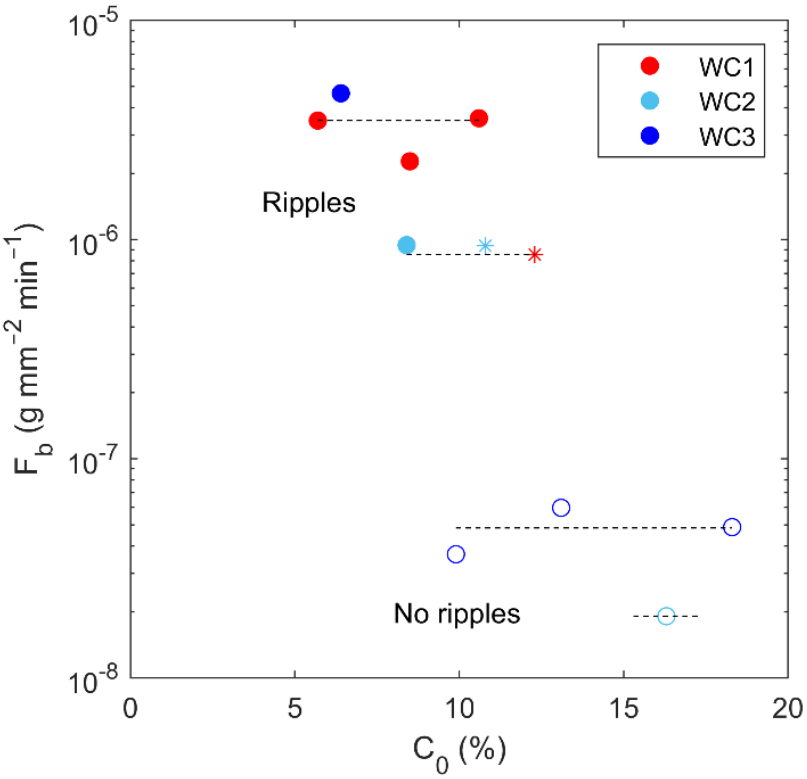

['Figure 8. Average clay mass flux out of the bed, F_b, against clay content, C_0, for WC1 (red; Wu et al., 2022), WC2 (light blue) and WC3 (dark blue). Here solid circles, asterisks and open circles signify large, small and no ripples.']

As regards the reviewer's concerns about the experimental configurations these are addressed below.

RC2, Anonymous (main comments)

I am sure that the authors meticulously design and run the experiments, but I have some concerns about their experiment configurations, which can affect experimental condition characterization and results. Please see below for the details.

(1) The experiments were conducted in a recirculating flume tank, where two different types of sediment are placed in the streamwise direction (mixed sand clay in upstream and clean sand downstream). In such configuration, only clean sand is likely to be recirculated during the experiments, which can change clay – sand mixture ratio in the test section. Although the authors argue the decreases in clay content after the experiments in Figure 5 are mainly associated with clay winnowing, the decreases in clay content can be also affected by the recirculated sand. Was the recirculated sand transport rate measured and negligibly small? More explanations are needed in this matter.

We agree with the Reviewer that a fraction of clean sand was recirculated during the course of the experiments. Based on the largest grains in suspension, determined by a settling velocity associated with the skin friction (Fredsøe and Deigaard, 1992, doi: 10.1142/1546), we estimate it to be about 1% of the sand grains on the bed in the clean-sand section. We believe that the recirculation of this clean-sand fraction has a negligible effect on the dilution of clay content in the mixed sand-clay section. This is demonstrated by the vertical consistency in clay content observed in post-experiment sediment cores collected from the flat beds (f – h, and k in Figure 5), where the mixed sections were below threshold, but the clean-sand section was above

threshold. Had there been a substantial effect in these cases the cores would have shown some vertical variation.

(2) I presume the flume is separated with the brick walls to maximize the number of experiments in one run. The height of the brick walls (0.2 m) is a half of the water depth (0.4 m). Why is it not entirely separated (the height of the brick walls > 0.4 m)? I can imagine that some three-dimensional flow structures are generated at the interface between top (> 0.2 m) and bottom (< 0.2 m) layers, which would not exist in normal flow conditions (i.e. without flume separations). Did authors check vertical velocity profiles before flume separation are comparable with the ones obtained after flume separation? If there are substantial differences between the velocity profiles, quite different bed shear stress can be obtained even with the same experiment conditions. This can affect your 3D phase diagram.

The brick walls were indeed used to maximise the number of experiments for each run. In these experiments and those of Wu et al. (2022), short walls were chosen for two reason: (i) to help ensure flow was more consistent across the tank as a whole between channels and (ii) so that it possible to take sediment cores during the experiment when the flow was temporarily paused. We acknowledge that this short-wall configuration could potentially induce the development of 3D flow structures, but we did not take any velocity measurements prior to putting the walls in place for practical reasons (the walls were built before the sediment was added). Nonetheless, we presumed that this 3D flow pattern would be minimal. This presumption is supported by the consistent and conventional, cross-channel ripple structure for both 2D and 3D ripples (see Figure 4). Moreover, our results show a greater tendency towards 2D straight-crested ripples than other experiments (L286-292). As far as the 3D phase diagram is concerned, each channel had its own hydrodynamic measurement determined along the centre line where any 3D flow effect would be the least possible.

(3) Also, regarding the flume separation, there seems to be a preferential bed slope that can affect ripple development. For example, more sediment aggregation (larger ripples) is observed in the upper part of the panel c,f (channel 3) in Figure 4. Similarly, more sediment aggregation (larger ripples) is observed in the lower part of the panel b,d (channel 1) in Figure 4. This can influence ripple morphology characterization (particularly height and steepness). Some explanations are needed in this matter.

We believe that sediment aggregation was mainly due to a degree of wave reflection despite wave absorption at the downstream end of the flume by the artificial beach. It may also be related to competing patches, where wave ripples first form, spreading out and interacting with one another (Sekiguchi and Sunamura, 2004, doi: 10.1016/j.coastaleng.2003.11.002). Similar behaviours have been reported previously within this wave tank (Wu et al., 2018, doi:10.1029/2018JF004681). However, our approach involved the recording of ripple data through URS sensors across the entire channel within a 2-meter URS-scanning area to capture the average ripple development characteristics. This methodology effectively mitigated the potential influence of uneven sediment aggregation. A phrase has been added to L153 to make this clearer. Most importantly, as depicted in Figure 6a, there is a consistent trend in ripple steepness for larger ripples as the clay content increased from 0 to 10.8%. It also suggests that the impact of both wall-induced 3D flow structures, as mentioned above, and wave reflections on ripple geometries is negligible.

[L 153: 'calculation of the mean, across-channel values of λ_t and η_t at a bed scanning …']

(4) Lastly, the test section is located fairly close to the current inlet (only ~ 2 times of the channel width excluding the gravel section). I wonder whether the space is enough for the flow to fully develop. If the flow is still in transition (not fully developed), this can explain why

slightly inhomogeneous ripple fields are generated in different channels that are described above. Please address this matter if the authors have checked the flow is fully developed.
Based on the work of Elliot (1958), doi:10.1029/TR039i006p01048, in response to a change in roughness from skin friction, $z_0 = 2.5D_{50}/30 = D_{50}/12$, to form drag, $z_0 \sim \eta_e^2/\lambda_e$, the distance along the tank for full boundary layer development in water depth of 0.4 m is 0.28 m, so the 1-m gravel section is sufficient.

RC2, Anonymous (specific comments)
(5) In the abstract, please avoid speculative words, such as "likely associated with hydraulic conductivity" or "which may be significant for paleoenvironmental reconstruction". I further wonder whether readers can understand the reason of your findings at this stage. It could be worth skipping such explanations and leaving them for the discussion section.
We would argue that the first example using 'likely' to describe an effect is not speculative, particularly as we have now made it more specific in L18 – 19:
['… C_0 > 10.6%, likely associated with a 3-orders of magnitude decrease in hydraulic conductivity.']

However, we accept that the second example is speculative and so have removed it.
[L 20-21: 'linear decrease in wavelength with C_0 for C_0 > 7.4%. Moreover, for a given flow, …']

(6) L29-30: In the introduction, please define combined wave-current flows before using it.
We have introduced the definition of combined flow at the beginning of the introduction:
[L29-31: 'In coastal and estuarine environments, the superimposition of waves and currents, termed combined wave–current flows, are a common occurrence. In these environments, which include continental shelves, the shoreface, and tidal flats, combined wave–current flows frequently form ripples on the seabed (e.g., Osborne and Greenwood, 1993; …']

(7) L74-77: Importance of point (1) and (2) is not clearly stated in the introduction. I also think point (3) is the main scientific contribution of this paper. Please consider putting point (3) first.
We have restructured the introduction to emphasize the significance of points 1 and 2. The revised introduction also underscores the importance of understanding points 1 and 2 as fundamental prerequisites for addressing point 3(see the revised introduction at the end of this document).

(8) L83: temporal resolution of the velocity measurement looks low. From my understanding, Vectrino profiler can collect velocity samples up to 200 Hz. Is there any reason of low temporal resolution? If there is, please explain it in the revised manuscript.
The purpose of measuring the velocity in the experiments is to obtain the average velocity necessary for determining skin friction using Malarkey and Davies' (2013) method as we mentioned in L121. Consequently, variations in the ADV sampling frequency do not impact the results of the mean data. Hence, we opted to use a sampling frequency of 25 Hz in these experiments.

(9) L83: please also provide the velocity measurement duration.
We have added this information:
[L83: '…flow velocities in each channel were measured by a 25 Hz Vectrino profiler throughout the entire duration of the experiments.']

(10) Please consider change notation of wave velocity magnitude U0 into Uw for the sake of readability.
We accept this, particularly as it is more consistent with θ_w, particularly as θ_0 is used for the clean-sand threshold of motion, and so will change U_0 to U_w where it appears.

(11) L103: please elaborate how C0 is measured? Is it based on mass or volume? If it is based on the volume, how the bed porosity is considered?
C_0 is based on mass. This has been clarified in the text.
['…, and Run 2, with C_0 of 9.9%, 13.1%, and 18.3% by dry weight in channels 1 to 3…']

(12) L115-116: please explain how you define "sufficiently not well mixed channel" Is it based on visual inspection? Or is it based on inhomogeneous ripple development?
This was determined through core samples which has now been added to the text.
[… because core samples collected from the flat bed showed that the sediment in this channel …]

(13) Please consider rearrange the order of experiments in Table 1. Consistent grouping based on experimental parameters seems to me more important than chronological order. To be specific, it would be better to present results of WC3 in an order of increasing C0.
We believe presenting the experimental process in chronological order is essential for the reader's understanding, as it helps illustrate how the experiments were conducted; relying on the natural winnowing of the bed, as explained above in response to Reviewer 1. Table 2, and indeed Tables A1-A3, all of which list ripple characteristic rather than flow parameters, are arranged by flow type and in increasing order of C_0, so that trends can be picked out more readily.

(14) Please consider putting experimental parameters of the WC1 experiments in Table 1. Please clearly state that the WC1 results are from Wu et al. (2022).
We believe Table A1 is a more suitable location for the WC1 experiments as it helps clarify that the WC1 experiments are taken from Wu et al. (2022) and separate from the present experiments but with the same experimental setup. However we agree that incorporating a summarized overview of the parameters used in the WC1 experiments within Table 1 would significantly enhance readability. Consequently, we have expanded the note 1 following Table 1 to accommodate this additional information:
['… and WC3 is the strongest. For WC1 (Table A1), corresponding to $0 \leq C_0 \leq 12.6$, $0.31 \leq U_w \leq 0.33$ m/s, $0.15 \leq U_c \leq 0.2$ m/s, $0.15 \leq \theta_w \leq 0.16$ and $0.007 \leq \theta_c \leq 0.13$, ripples under WC1 conditions always developed.']

We also have made the text more explicit:
[L96-97: 'The wave–current flow conditions (WC1, in Table A1 from Wu et al., 2022; WC2 and WC3, in Table 1) are numbered according to increasing relative current strength, from the weakest, WC1 to the strongest, WC3. The experiments involved …'
L146-147: '[1]The flow code represents the relative current strength, where WC1 (Wu et al., 2022, Table A1) is the weakest and WC3 is the strongest.']

(15) Figure 2: If I am not mistaken, WC1 results are from Wu et al. (2022). Please clearly state this. Also, last tick of 0.25 in the x-axis is cut out in Figure 2.

Both of these issues have been rectified.

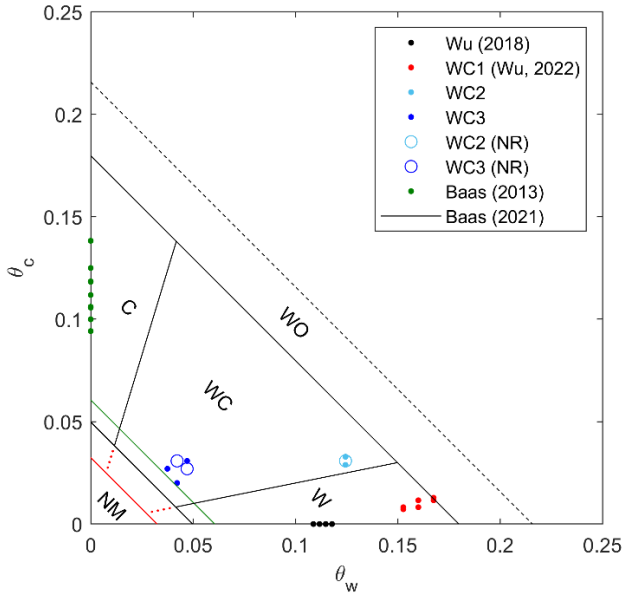

[L173: '(Wu et al., 2018), wave-current, WC1 (Wu et al., 2022), WC2 and WC3, and current-…]

(16) L260: Please discuss how the threshold of C0 ~ 10 % will change under saline water (more realistic flow condition in coastal regions), not freshwater.

The data of Wu et al. (2018) experiments, see Table A3, were performed in salt water. While these experiments do not cover a very wide a range of clay concentrations, $0 \leq C_0 \leq 7.4\%$, the fact that these experiments are consistent with all the other freshwater experiments leads us to believe that if there is an effect it is likely to be very weak. In addition, our argument that hydraulic conductivity drops significantly at ~10% does not depend on the presence of salt or fresh water.

Restructured Introduction and Conclusions

1 Introduction

In coastal and estuarine environments, the superimposition of waves and currents, termed combined wave–current flows, is a common occurrence. In these environments, which include continental shelves, the shoreface, and tidal flats, combined wave–current flows frequently form ripples on the seabed (e.g., Osborne and Greenwood, 1993; Li and Amos, 1999; Héquette et al., 2008; Gao, 2019). Ripple dynamics play a crucial role in sediment transport, which in turn affects the predictions of large-scale coastal morphodynamic numerical models (Brakenhoff et al., 2020), the underwater scour around civil engineering structures (Sumer et al., 2001), and the transport of nutrients and contaminants (Vercruysse et al., 2017). Moreover, combined-flow ripples have been found in the geological record, thus providing key information for reconstructing paleoenvironments (e.g., Myrow et al., 2006, Beard et al., 2017). It is therefore crucial to examine how combined-flow hydrodynamics control ripple dimensions and vice versa, particularly in muddy coastal and estuarine environments that are widespread in nature (Healy et al., 2002) and characterised by sediment consisting of a mixture of cohesive clay and non-cohesive sand. A full understanding of this process will ultimately prove significant for coastal and estuarine management and ecological balance maintenance,

especially as such areas may face more extreme weather events in the context of climate change and sea level rise (e.g., Mousavi et al., 2011, Vitousek et al., 2017).

To date, however, there has been a scarcity of relevant literature on this topic. Wu et al. (2022) were the first to consider ripple dynamics in sand–clay mixtures under combined flows. Their study showed that small flat ripples formed for initial clay contents, C_0, greater than 10.6% under hydrodynamic conditions that formed large equilibrium ripples in clean sand. Moreover, Wu et al. (2022) demonstrated that clay winnowing efficiency plays a significant role in the development towards clean-sand-like ripples on mixed sand–clay beds. They also highlighted the process of deep cleaning of clay below ripple troughs for $C_0 \leq 10.6\%$, whereas Wu et al. (2018) revealed a more modest deep accumulation of clay beneath rippled beds under wave-alone conditions for $C_0 \leq 7.4\%$. This suggests a dynamic balance between loss and accumulation of clay during ripple development. However, the key factors governing this dynamic balance, and the resulting ripple size, remain unclear, primarily due to the limited number of flow conditions considered thus far. This knowledge deficiency in mixed sand–clay experiments is reflected in the existing ripple predictors, i.e., bedform phase diagrams and empirical formulae, that are based exclusively on clean-sand experiments.

Phase diagrams group similar bedform types and cross-sectional geometries for known hydrodynamic conditions and sediment properties (e.g., Van den Berg and Van Gelder, 1993). In the last thirty years, a substantial number of experimental studies has made progress in compiling combined-flow ripple phase diagrams (Arnott and Southard, 1990, Kleinhans, 2005, Dumas et al., 2005, Cummings et al., 2009, Perillo et al., 2014). Using a range of combined-flow conditions in an experimental flume, Perillo et al. (2014) expanded the bedform phase diagrams of Arnott and Southard (1990) and Dumas et al. (2005) by subdividing bedform types based on planform geometry. Baas et al.'s (2021) phase diagram, based on field observations of bedforms on an intertidal flat in the Dee Estuary, U.K., captured bedform types generated under a wider range of flow conditions, including those generated under waves and currents at angles to one another. Compared to wave-alone and current-alone ripple predictors, relatively few predictors are available for combined flow ripples. Tanaka and Dang (1996) modified a widely used predictor for wave ripples developed by Wiberg and Harris (1994) by considering the influence of grain size and the relative strength of the wave and current velocities on the ripple size. Khelifa and Ouellet (2000) developed a new formulation to predict ripple dimensions by introducing an effective combined-flow mobility parameter.

The experiments of Wu et al. (2022) were conducted under a single wave-dominated combined-flow condition, but further study considering wider hydrodynamic conditions are required for a more comprehensive understanding of the interaction between ripple development and winnowing-induced clay loss from beds. These insights are critical for the development of morphodynamic models applicable in muddy estuaries and the coastal zone. Therefore, the present study extends Wu et al.'s (2022) experiments and describes a systematically collected set of data from large-scale flume experiments on ripple development. This study also draws in available sand–clay experiments under current-alone and wave-alone conditions (Baas et al., 2013; Wu et al, 2018). The three specific objectives of this study were: (1) to compare ripple development and occurrence on beds with similar initial clay contents under different hydrodynamic conditions; (2) to compare clay winnowing efficiency during ripple development, under different flow conditions; and (3) to propose a new phase diagram for bedforms generated in sand–clay substrates to systematise the experiments, using the knowledge gained from objectives 1 and 2.

Conclusions

The present experiments examined ripple dynamics on cohesive beds under two different combined wave–current conditions with initial clay content, C_0, in the range from 0 to 18.3%.

For the lowest C_0, these experiments produced quasi-asymmetric ripples, which are similar to their clean sand counterparts, with heights and wavelengths in the range $13.9 \leq \eta_e \leq 15$ mm and $137 \leq \lambda_e \leq 148$ mm, respectively, with the larger values corresponding to the strongest relative current, WC3. For higher C_0, smaller flatter ripples that were fully asymmetric, with $\eta_e = 5.6$ mm and $\lambda_e = 125$ mm, were produced. Finally, for the highest C_0, no ripples were produced and the bed remained flat.

Combining the present experiments with previous wave-only and wave–current experiments (Wu et al., 2018; 2022) demonstrates the existence of a large to small equilibrium ripple discontinuity at $C_0 = 10.6\%$, with two distinct ripple steepness (RS) groupings, RS ≥ 0.09 and RS ≈ 0.04, which is probably related to a three-orders of magnitude decrease in the hydraulic conductivity. The larger RS grouping shows a decrease from 0.14 to 0.1 with increasing current strength. Ripple wavelength was independent of initial clay content for $C_0 \leq 7.4\%$, but it decreased linearly with initial clay content for $C_0 > 7.4\%$. For $C_0 \leq 7.4\%$, the wavelength was proportional to the current-enhanced orbital diameter, d_{wc}, so that $\lambda_e = \alpha d_{wc}$, where $\alpha = 0.61$. For $C_0 > 7.4\%$, α decreased linearly, which could be important for paleoenvironment reconstruction, when λ_e is measured and d_{wc} is unknown. During the experiments, winnowing removed clay from both the active layer (crest to trough) and deep beneath it, in the case of most large ripples. Winnowing was quantified by the average mass flux of clay out of the bed over the duration of the experiments. Winnowing still occurred from flat beds, but compared to the large ripples the flux was typically two orders of magnitude smaller.

The ripple initiation time increased with initial clay content, and ultimately the bed remained flat when the initial clay content was large enough, demonstrating the enhancement of the threshold of sediment motion with increased initial clay content. When combined with the fine-sand, current-only experimental results of Baas et al. (2013), this allowed the enhancement of the threshold to be quantified for both coarse ($0.45 \leq D_{50} \leq 0.5$ mm) and fine ($D_{50} = 0.143$ mm) mixed sand–clay motion. On the basis of these enhancements, new 3D phase diagrams, involving the non-dimensional wave and current shear stresses and C_0 are proposed to characterise the two ripple size groupings under different flow conditions. This new 3D phase diagram framework should prove important to the morphodynamic modelling community.